STUDIA UBB CHEMIA, LXVIII, 2, 2023 (p. 53-71)
(RECOMMENDED CITATION)
DOI:10.24193/subbchem.2023.2.04

STABLE AND EFFICIENT BIOPOLYMERIC NANOCOMPOZITE OF *CANDIDA ANTARCTICA* LIPASE B

Cristina-Georgiana SPELMEZAN[a], Alin BACOȘ[a], Gabriel KATONA[a]

ABSTRACT. The catalytic performance of various biocatalysts obtained by the adsorption of lipase B from *Candida antarctica* (CaL-B) onto and into polyvinyl alcohol (PVA) and polylactic acid (PLA) nanofibers were tested in the kinetic resolution of racemic 1-benzo[b]thiophen-2-yl-ethanol by transesterification. Best performance regarding reaction velocity and selectivity was registered for CaL-B adsorbed onto PLA nanofibers. The high operational stability of this biocatalyst was confirmed in recycling experiments, after 5 cycles the biocatalyst maintained 86.6% of its initial activity. The optimal process parameters in continuous flow mode also were established.

Keywords: *CaL-B, nanofibers, polyvinyl alcohol, polylactic acid, EKR*

INTRODUCTION

Along with the industrial development of biotechnologies, a much convenient approaches for a wide range of processes, the need for stable and active biocatalysts with superior properties increases. The immobilization of enzymes was perceived as an excellent method in order to improve their availability and allows the reuse to provide higher productivity [1].

There are many reasons why the enzymes in their immobilized form are preferred, such as: reduction of the technological process complexity due to the increasing variety of bioreactors that can be used, easier separation

[a] *Babeş-Bolyai University, Faculty of Chemistry and Chemical Engineering, 11 Arany Janos str., RO-400028, Cluj-Napoca, Romania*
* *Corresponding author: cristina.spelmezan@ubbcluj.ro*

from the reaction mixture, higher stability to environmental changes (pH, temperature) and an impressive improved stability in organic solvents with an increased activity [2-4].

Besides the advantages of using immobilized enzymes, there are also some disadvantages: the fragility of the supports, possible decrease or even disappearance of the enzyme activity after immobilization, especially when covalent bonds are involved. Most of these shortcomings can be eliminated by focusing on new, innovative supports and the correct choice of the immobilization method [5-7].

The material used as support for the immobilization must allow a high enzyme loading, it needs to have a surface/volume *ratio* as high as possible, to be stable in the reaction media, and to be chemically inert in relation to the reactants and products [1]. Inorganic materials, synthetic organic polymers or biopolymers can be used as support. One of the important factors in the choice of the support is the ecological aspect, which led to the gradual transition from the first two categories to the biopolymers [7]. Materials with nanometer dimensions (nanoparticles, nanotubes or nanocomposites) present a major interest in the immobilization field, due to their high surface/volume *ratio*, since they have a great potential for controlling enzymes environment, enhancing the enzyme activity and operational stability. Until recently, these supports were considered the most promising for the optimization of classical biocatalysts, since they can lower the mass transfer limitations due to the high dispersion in the reaction medium; however, in order to reduce the difficulty to recover the biocatalyst at the end of the enzymatic reaction, the efforts were focused on other nanomaterials of biopolymeric nature [7].

Biopolymer nanofibers possess a great potential to reduce these constraints, since they facilitate the contact between the catalyst and the substrate on very large area. The most used method for obtaining nanofibers is the electrospinning technique, allowing the facile solvent removal during the manufacturing process. Since the nanoparticles are tough to disperse into solution and further to recover and to reuse them, nanofibers can be easily separated and reused in batch system or applied in continuous flow mode [8-10]. Moreover, the enzyme is immobilized into the network of the nanofibers, therefore its spatial structure does not suffer modifications, being more stable at high temperature or extreme pH values, finally improving the biocatalyst efficiency [9,10].

Many biopolymers such as polylactic acid (PLA), polycaprolactone (PCL), chitosan (CS) and polyvinyl alcohol (PVA) are used for the production of nanofibers through electrospinning technique [11-15].

Polylactic acid (PLA), is used as an alternative material for different biomedical applications, such as: artificial skin, drug delivery materials, packaging and tissue engineering, because it is renewable, biodegradable, biocompatible and energy-saving [16-22].

Poly(vinyl alcohol) (PVA), is a hydrophilic, biocompatible, non-toxic semicrystalline polymer, with properties like: thermal stability, strength, water solubility and permeability [23,24]. This polymer is also used for different biomedical applications, such as: tissue engineering, packaging. The major downfall of PVA nanofibers, is that an additional step is necessary prior using the nanofibers in enzymatic kinetic resolution when the reaction medium is water. Usually, the nanofibers are reticulated using glutaraldehyde vapors [23].

During the last 30 years, lipases have become the most used enzymes for commercial applications. In the large scale bioprocesses, beside their catalytic activity, the catalysts operational stability is highly important, and along with the modulation of enzymes selectivity and activity, the necessity to improve the stability of the enzymes and to convert them into stable, robust, recyclable catalysts, has become critical [25-31].

Lipase B from *Candida antarctica* (CaL-B) has a high lipolytic activity [30,31] and is used in the biomedical field [32-40]. Based on its well-known properties (absolute selectivity, affinity towards different substrates, high stability to high temperatures and organic solvents) [41-43], CaL-B was reported to be an efficient catalyst in the EKR processes of secondary racemic ethanols [14,44], permitting us to obtain both enantiomerically pure stereoisomers [45-48]. As a part of our interest to develop biocatalysts for the preparation of optically active ethanols bearing a heteroaromatic moiety as important chiral building blocks in the stereoselective drug synthesis [49,50] or for different compounds with antibacterial activity [51], we turned our attention to the lipase immobilization using as support biopolymeric nanofibres. 1-benzo[*b*]thiophen-2-yl-ethanol was chosen as model compound, since it is the key intermediate for the synthesis of Zileuton, a 5-lipoxygenase inhibitor which is also used in asthma medication [52].

Although immobilization of enzymes in PVA and PLA is known, our aim was to evaluate and improve the activity and reusability of lipase biocatalyst membrane. In the current paper, the lipase B from *Candida antarctica* was immobilized onto biopolymeric nanofibers of polylactic acid (PLA) and polyvinyl alcohol (PVA) prepared by electrospinning by adsorption or entrapment and further tested for the enzymatic kinetic resolution of *rac*-1-benzo[*b*]thiophen-2-yl-ethanol in discontinuous and continuous systems.

RESULTS AND DISCUSSION

The nanofibers morphology

The obtained nanofibers were analyzed by electronic transmission microscope. The nanometric dimensions of the fibers were confirmed by TEM images, with diameter between 126 and 439 nm (Figure 1a). In the images recorded before (Figure 1b) and after (Figure 1c) the immobilization of CaL-B onto PLA nanofibers, structural changes, confirming the presence of enzyme molecules at the surface of the nanofibers, were observed as irregular conglomerates on the nanofibers surface.

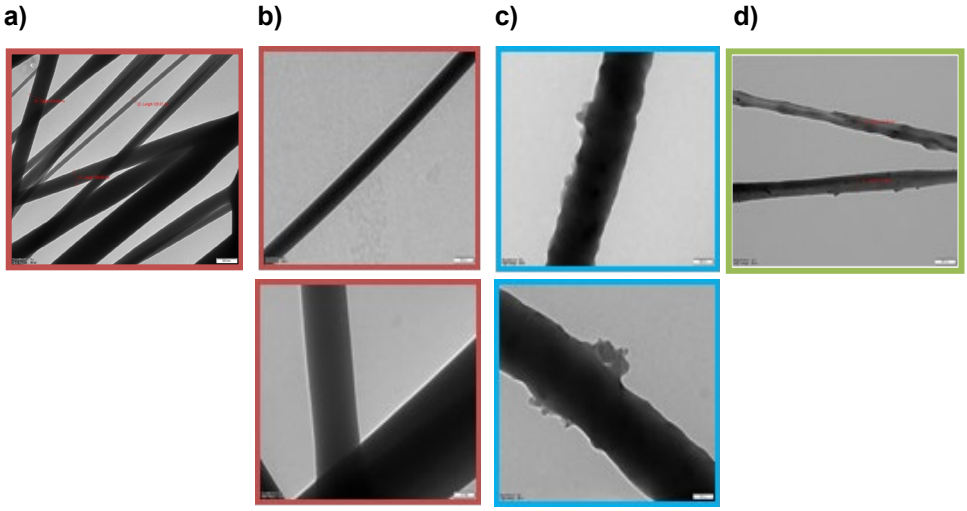

Figure 1. a) PLA fibers length in the range 126-439 nm, using a magnification of 6× (500 nm) and high voltage (80kV); **b)** PLA nanofibers homogenity and uniform distribution, with a magnification of 20× (100 nm) and high voltage (80kV); **c)** TEM images of the new biocatalyst PLA nanofibers with CaL-B adsorbed on their surface, with a magnification of 20× (100 nm) and high voltage (80kV); **d)** TEM image of PVA based biocatalyst, using a magnification of 10× (200 nm) and a high voltage of 80 kV.

Cal-B immobilization by adsorption and entrapment in PLA and PVA nanofibers

At industrial level, the most used immobilization techniques are: physical adsorption, inclusion, cross-linking and covalent bonding, the first two being preferred due to the price-cost efficiency *ratio*. Cross-linking involves

both inclusion and covalent bonding through the use of specific chemical agents, most often glutaraldehyde vapors. Due to the prevalence of these methods, the recent research has focused especially on the adsorption and encapsulation as immobilization methods [7,53].

Physical adsorption is simple and cheap, the obtained biocatalyst presents a high catalytic activity, the enzyme does not suffer any conformational changes and there is no need to use reagents. Even if this method has the previous advantages, it also presents some disadvantages, such as: low stability, possible loss or desorption of the enzyme, due to the weak bonds.

The method that uses the entrapment of the enzyme protects the biocatalyst, allows the transport of low molecular weight compounds, can be used in a continuous regime, can be easily separated from the reaction medium, and allows controlled release of the product. The downfall of this type of immobilization is represented by the limitations on the mass transfer and a low enzyme loading [6].

Chemical synthesis of model compound

Racemic 1-benzo[*b*]thiophen-2-yl-ethanol (*rac*-**2**) was synthetized by Grignard reaction from its corresponding aldehyde (**1**) and further used as substrate in the *O*-transesterification reactions and as starting material for the chemical synthesis of its corresponding acetate (*rac*-**3**) (Scheme a,b).

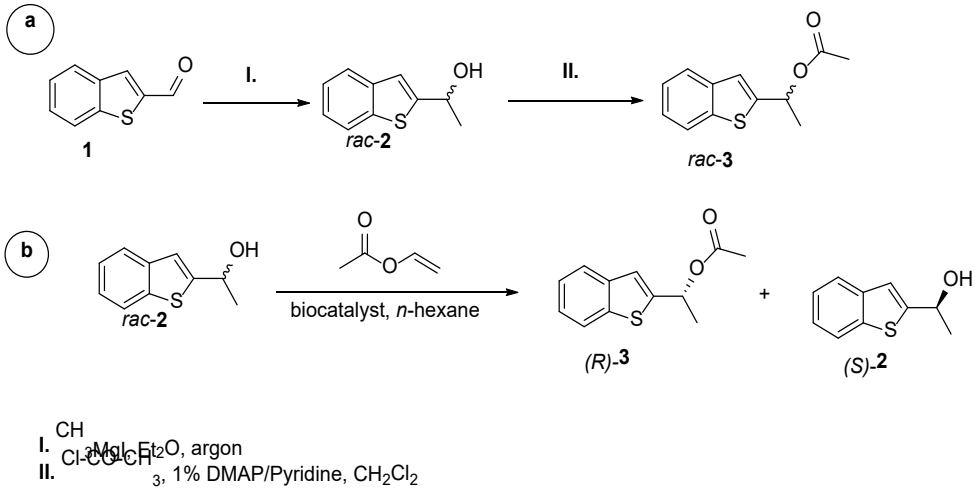

Scheme 1. a. Chemical synthesis of racemic compounds; **b.** EKR of racemic 1-benzo[*b*]thiophen-2-yl-ethanol by lipase catalyzed enantioselective transesterification.

EKR of racemic 1-benzo[*b*]thiophen-2-yl-ethanol in discontinuous system PVA nanofibers based biocatalysts

The efficiency of the obtained biocatalysts was tested in the enantioselective *O*-transesterification of *rac*-1-benzo[*b*]thiophen-2-yl-ethanol with vinyl acetate. First, in order to maximize the productivity, the process was performed under the same conditions: 4 equiv. of acylating agent, 1 mL of *n*-hexane, and two substrate: enzyme weight *ratios* 8:1 and 10:1. Samples were taken periodically, every 2h, until the reaction reached the maximum conversion of 50% (Figure 2). The obtained results show an optimum substrate: enzyme weight *ratio* 8:1, therefore, for the next experiments this *ratio* was used.

Further, we investigated the influence of substrate: vinyl acetate molar *ratio* over the reaction rate. For these experiments, we tested the already known amount of vinyl acetate from previous studies (2 equiv.) [14] and the one that we have used (4 equiv.). The reactions were monitored, by taking samples every 2h until the maximum conversion was reached. As already determined, the best biocatalyst reached the 50% conversion after eight hours when 4 equiv. of vinyl acetate were used. In the reaction were 2 equiv. were used, after eight hours the reaction reached only a conversion of 36.8%.

In the case of the lipase adsorbed on PVA 12% nanofibers, lower conversion were obtained. The cause can be both the high polymer concentration, which limits the mass transfer, making the substrate access to the enzyme catalytic site more difficult, but also the high enzyme loading which can lead to the enzyme conglomerates formation.

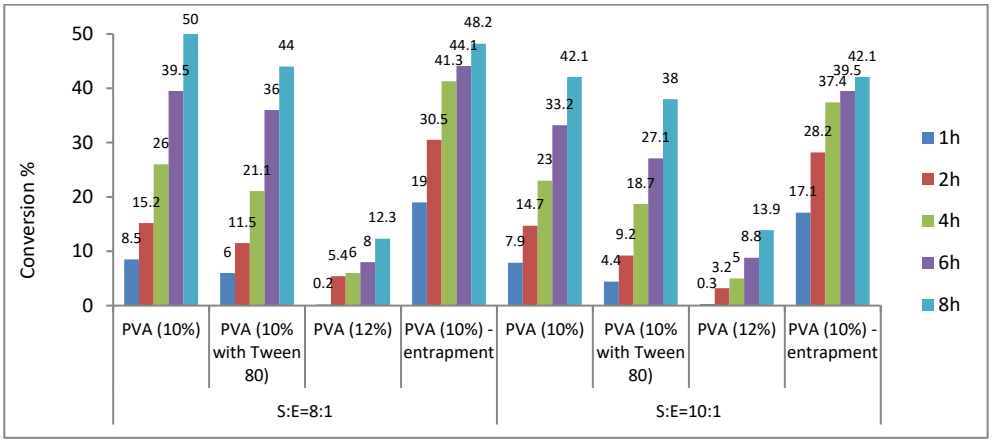

Figure 2. The influence of substrate:enzyme weight *ratio* on the transesterification of model compound with vinyl acetate (4 equiv. in *n*-hexane at 30°C and 1000 rpm, during 8h) mediated by PVA based biocatalysts.

PLA nanofibers based biocatalysts

A preliminary determination of substrate:vinyl acetate molar ratio was done. Therefore, we used two amounts of acylating agent: 2 and 4 equiv. We expected that the 4 equiv. to be the optimal molar *ratio* as it was in the case of the biocatalyst based on PVA nanofibers, but for the enzymatic preparate based on PLA nanofibers the optimal molar *ratio* was 2 equiv. of vinyl acetate, obtaining the maximum conversion in 1.5 hours, compared to the experiment where 4 equiv. were used, and the reaction was completed only after 6 hours.

Next, the EKR was performed under the same conditions using 2 equiv. of acylating agent, 1 mL of *n*-hexane, and a substrate : enzyme weight *ratio* 8:1 with the PLA based biocatalyst prepared by both, adsorption and entrapment methods. Samples were taken periodically, until the reaction reached the maximum conversion. Since the use of CaL-B adsorbed biocatalyst allows the maximal 50% conversion in 1.5h, the recycling experiments were performed with this biocatalyst (Figure 3).

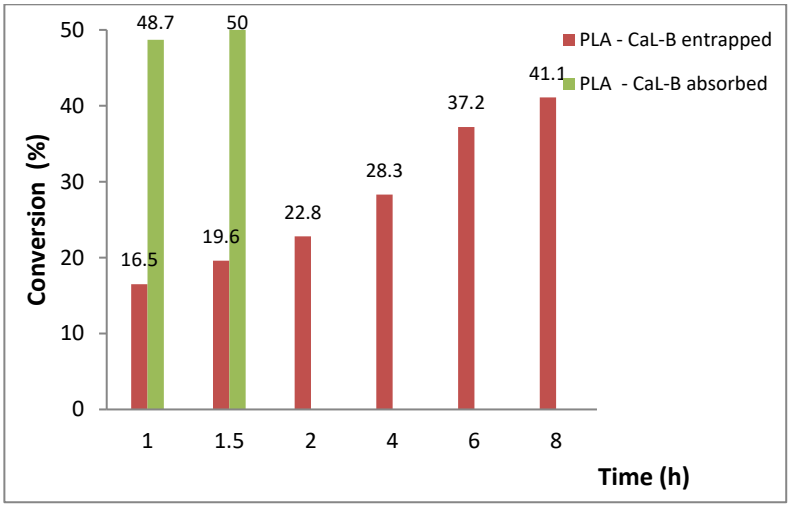

Figure 3. The influence of the immobilization method on the *O*-transesterification of racemic alcohol with vinyl acetate mediated by PLA based biocatalysts (2 equiv. in *n*-hexane at 30°C and 1000 rpm).

As presented in Figure 3, the CaL-B adsorbed has proven to be more efficient the EKR of the model compound, reaching the maximum 50% conversion in 1.5h, while for the same lipase immobilized by entrapment a 41% conversion

was recorded only after 8h. In order to explain these results, the biocatalyst prepared by entrapment was analyzed by scanning electron microscopy, a very compact structure being observed. A possible explanation is the reduced mobility of enzyme molecules trapped in the polymeric lattice, which led to a much smaller activity, resulting in a decreased reaction rate. Furthermore, in order to access the catalytic site, the substrate molecules need to over-cross the polymeric hydrophobic membrane which is able to interact with the substrate.

The entrapment of lipase in PLA nanofibers described in the literature [54], led in our experiments to a compact structure (Figure 4), which does not allow the organic compound diffusion in order to reach the entrapped enzyme.

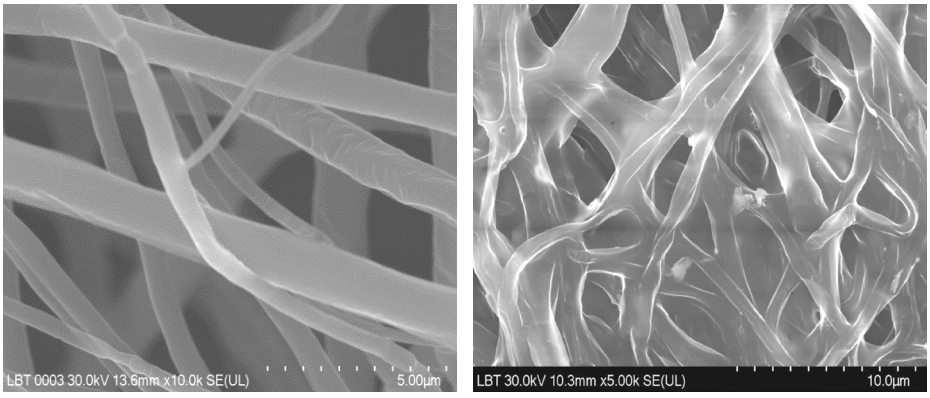

Figure 4. SEM images of PLA nanofibers without and with entrapped CaL-B molecules, showing a compact structure.

Recycling experiments

The recycling represents a crucial condition in any process, permitting the development of sustainable technologies. Further, the reusability of the most promising CaL-B bioconjugate was studied in the enantioselective acylation of racemic 1-benzo[*b*]thiophen-2-yl-ethanol with vinyl acetate. As presented in Figure 5, the activity of the enzymatic preparate remains relatively high after 10 cycles, decreasing by 12%. As effect, the operational and long stability makes this biocatalyst promising in the continuous-flow system, permitting a higher productivity.

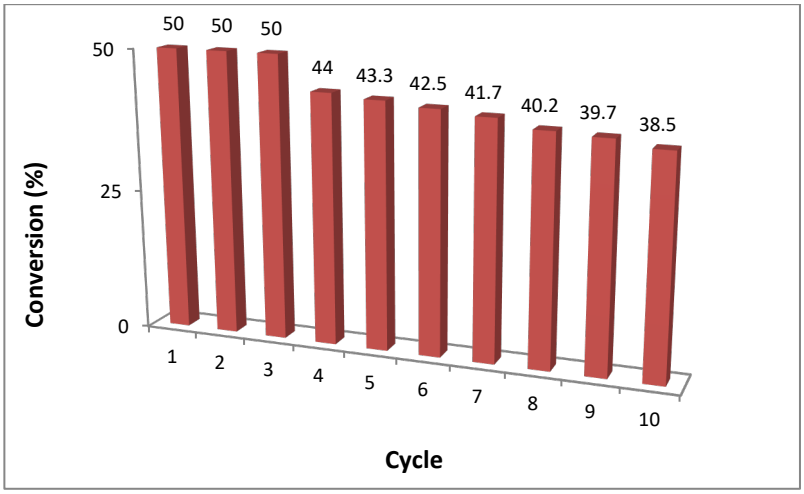

Figure 5. The reusability of PLA-CaL-B prepared by adsorption in the EKR of *rac*-1-benzo[*b*]thiophen-2-yl-ethanol (after 1h reaction time) with vinyl acetate (2 equiv.), in *n*-hexane at 30°C and 1000rpm.

EKR of racemic 1-benzo[*b*]thiophen-2-yl-ethanol in continuous system

The effects of two process parameters were studied: flow rate and temperature, maintaining the same concentration of substrate (8 mg/mL). The reaction progress was monitored taking samples periodically from the effluent and analyzing them by HPLC, until reaching the steady state conditions in the reactor (constant conversion). Experiments were performed at 30, 40, and 50°C, with 8 mg/mL substrate concentration solutions and flow rates in the range 0.2-0.5 mL/min (Figure 6).

At lower temperature (30°C) and 0.2–0.3 mL/min flow rate, the stationary regime was reached in short time (5–10 min), and high conversion (48.5 and 49% after 30 min), the biocatalyst providing a very good efficiency. Further, the influence of the temperature over the process was studied increasing it gradually with 10°C, expecting a higher conversion, in a shorter time. The maximum conversion was obtained after 4h for lower flow rates (0.2–0.3 mL/min). As conclusion, at 0.2–0.3 mL/min flow rates, an increased temperature is not justified, it will only increase the overall cost of the process.

In order to have the whole picture of the continuous regime, the flow rate was increased to 0.4–0.5 mL/min. As expected, lower conversion was noticed at 30°C (38% at 0.4 mL/min and 35% at 0.5 ml/min). Next, the flow

was maintained in this range increasing the temperature. We observed that the temperature plays an important role over the process conversion, but only at higher flow rate. For example, at 40°C the maximum 40% conversion was obtained at 0.4 mL/min), and 37% at 0.5 mL/min), while at 50°C, the highest conversions (43% for 0.4 mL/min and respectively 41% for 0.5 mL/min) were recorded.

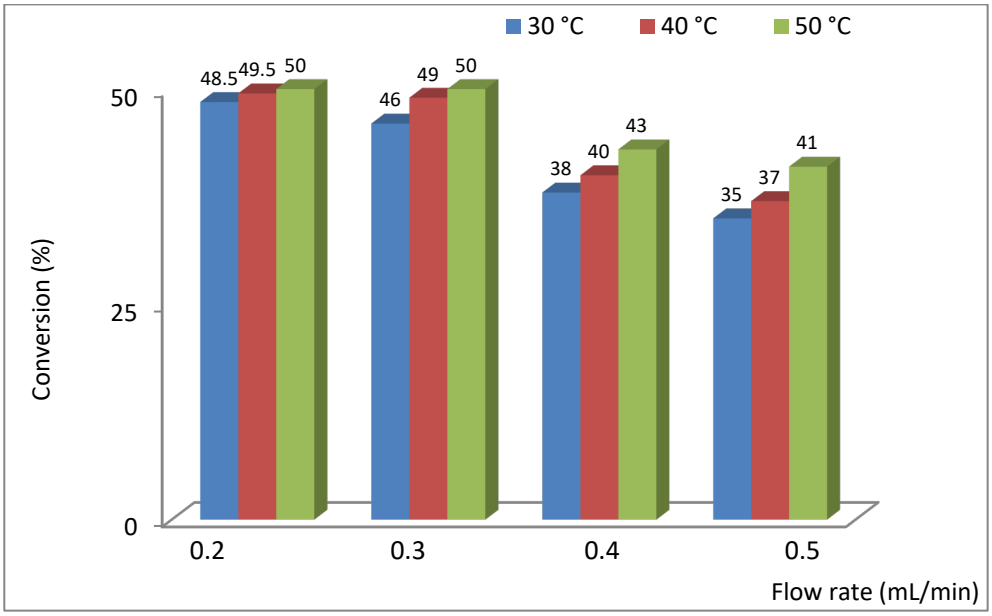

Figure 6. The influence of the temperature and flow rate in the EKR with CaL-B adsorbed on PLA-in continuous system (2 equiv. vinyl acetate, in *n*-hexane, 8 mg/mL substrate concentration; samples were withdrawn from the effluent after 30 min).

CONCLUSIONS

Our study demonstrated that the enzyme–nanofiber composite prepared by the adsorption of lipase B from *Candida antarctica* on PLA nanofibers obtained by electrospinning is an active and stable biocatalyst for the EKR of heteroarylethanols, important chiral building blocks. As compared with enzyme entrapment, this simple immobilization method implies simple operations and lower costs. In the recycling experiments in a batch system enzyme denaturation and the subsequent loss of activity were not observed, even after ten cycles the biocatalyst conserved 77% of the initial activity, making it promising for the development of continuous processes for an improved productivity.

EXPERIMENTAL SECTION

Materials and Instruments

Lipase B from *Candida antarctica* (CaL-B) was acquired in its free form (as a solution) from Novozymes (Copenhagen, Denmark) and dialyzed in double distilled water, followed by centrifugal concentration (using Amicon centrifugal filter, 33 kDa) to 15 mg/mL before use. Polyvinyl alcohol (PVA, molecular weight 130.000) and polylactic acid (PLA) were purchased from Sigma-Aldrich (Darmstadt, Germany). The reagents and solvents used in the enzymatic reactions were acquired from Sigma-Aldrich (Darmstadt, Germany) or VWR Chemicals (Darmstadt, Germany). Solvents for the chemical synthesis were used as procured (diethyl ether) or dried over molecular sieve (dichloromethane, chloroform and dimethylformamide).

For the manufacture of nanofibers, an electrospinning system Fluidnatek LE-50 purchased from Bioinicia (Paterna, Spain) was used.

The morphological analysis of the nanofibers was performed using a Hitachi H-7650 TEM electronic transmission microscope purchased from Hitachi Group (Tokyo, Japan) and Hitachi UHR-SEM 8230 also purchased from the Hitachi Group (Tokyo, Japan).

The thin layer chromatography (TLC) was performed on 0.2 mm Kieselgel sheets (Macherey-Nagel, Merck, Darmstadt, Germany) with UV-254 fluorescent indicator. Spots were visualized by treatment with 5% ethanolic phosphomolybdic acid, followed by heating. For all experiments, a Heidolph Vibramax 1000 shaker equipped with an incubator module (Heidolph, Schwabach, Germany) was used.

To determine the enzyme loading of the obtained biocatalyst, two methods were used for the quantitative analysis of protein solutions: the bicinchoninic acid (BCA Protein Assay) and Bradford kits. In both methods, the residual amount of enzyme in the solutions was performed by spectrophotometric quantification using a spectrophotometer Agilent 8453 Series purchased from Agilent (Waldbronn, Germany).

An Agilent 1200 Series HPLC purchased from Agilent (Waldbronn, Germany) was used for the quantitative analysis of the enzymatic kinetic resolution mixtures on LUX-i-Cellulose 5 (Cellulose tris(3,5-dichlorophenyl-carbamate) chiral column, 250 x 4.6 mm, 3 μm) from Phenomenex (Torrance, CA, USA) with 1 mL/min *n*-hexane-2-propanol mixture (95:5, v/v) as eluent. The conversion *c* was calculated with the Equation (1) using the enantiomeric excesses resulted from the peak area of substrate and product individual enantiomers [55].

$$c = \frac{ee_S}{ee_S + ee_P} \quad (1)$$

Electrospinning process

The electrospinning process was carry out at room temperature. The polymer solution was placed into a 10 mL syringe fitted with a stainless steel needle (3 cm long, 1 mm inner diameter). The flow rate was controlled with an automatic injection pump in the range 0.2–0.4 mL/h. A high voltage of 15–20 kV has been applied between the needle and the counter electrode collector wrapped with a thin aluminum foil having the a distance of 13–15 cm between the tip of the needle and the collector. The fibers were collected onto the counter collector for 4h and after were removed from the aluminum foil and left overnight to dry at room temperature prior using them in the further experiments.

Two PVA solutions (10 and 12 %) and one PLA solution (8%) were prepared by dissolving 1 or 1.2 g PVA crystals into distilled water (8 mL) and 0.8 g of PLA in 8 mL chloroform - dimethylformamide mixture (6:1, *v/v,* 8 mL) = 6:1 (*v/v*) and left under stirring at room temperature for 4h resulting in a clear solution, with occasional ultrasonic mixing. The final volume of each solution was corrected to 10 mL with the used solvent [54].

CaL-B immobilization through adsorption

The amount of lipase adsorbed to the polymeric nanofibers was calculated by measuring the protein concentration in the solution sampled before and after the immobilization procedures, including the unified wash-waters.

Immobilization of CaL-B onto PLA nanofibers

42.91 mg PLA 8% nanofibers, 1 mL lipase solution (15 mg/mL) and 2 mL phosphate buffer (pH=7.5) added for a better humectation of the fibers were mixed into a 5 mL tube and left under stirring at 4°C on orbital shaker for 28h [54]. The resulted biocatalyst (CaL-B adsorbed on PLA 8% nanofibers) was separated, washed with distilled water (2×2 mL), 2-propanol (2×2 mL) and *n*-hexane (1×1 mL) and dried at room temperature for 4h, resulting in a membrane with an enzyme loading of 7.6 %.

Adsorption of CaL-B onto PVA (10% and 12%) nanofibers

Due to its water-soluble properties, the lipase adsorption on PVA nanofibers requires a reticulation with glutaraldehyde [54]. For this additional step, the nanofibers collected on an aluminum foil were used as resulted in order to assure a higher surface for the contact with the reagent vapors. The foil was placed in a desiccator containing glutaraldehyde 25% solution. The PVA nanofibers were periodically checked for their solubility in water (at each 12h), until the nanofibers became completely insoluble, approximately after 3 days.

Further, 52.74 mg reticulated PVA10% or 46.81 mg reticulated PVA12% nanofibers, 1 mL enzyme solution (15 mg/mL) and 2 mL of phosphate buffer (pH=7.5) for a better fibers humectation were mixed into a 5 mL tube and left under stirring at 4°C on an orbital shaker for 28h [54]. The resulted biocatalyst (CaL-B adsorbed on reticulated PVA10% or PVA 12% nanofibers) was separated, washed with distilled water (3×2 mL) and dried at room temperature for 4h, resulting in membrane biocatalysts with 6.1 % and 9.5% respectively enzyme loading.

CaL-B immobilization through entrapment

The amount of immobilized lipase through entrapment into the polymeric nanofibers was calculated based on amounts of enzyme in the used solution and of nanofibers amount, considering a uniform enzyme distribution in the initial mixture.

CaL-B entrapment into PLA nanofibers

The mixture of PLA 8% solution (4 mL) and CaL-B solution (10 mg/mL, 0.25 mL) was left to homogenize for 25 min in the ultrasonic bath, loaded into the electrospinning syringe, and the process was performed at a high voltage of 19–20 kV and a needle tip-to-collector distance of 15 cm at a 0.4 mL/h flow, resulting in membrane biocatalysts with 0,78% enzyme loading.

CaL-B entrapment into PVA nanofibers

The mixture of PVA 10% solution (10 mL) and CaL-B solution (10 mg/mL, 1 mL) was left to homogenize for 10 min in the ultrasonic bath, loaded into the electrospinning syringe; the process was performed at a high voltage

of 15 kV, a distance of 13 cm between the needle tip-to-collector and a 0.25–0.3 mL/h flow [1], resulting in membrane biocatalysts with 1% enzyme loading.

Entrapment of CaL-B into PVA 10% nanofibers in the presence of Tween 80

The mixture of PVA 10% solution (10 mL) and CaL-B solution (10 mg/mL, 1 mL) and of Tween 80 solution (1% *v/v,* 60 µL) was left to homogenize in the ultrasonic bath for 25 min, loaded into the electrospinning syringe, and the process was performed at a high voltage of 15 kV, a distance of 13 cm needle tip-to-collector and 0.2 mL/h flow, resulting in membrane biocatalysts with approx. 1% enzyme loading.

Although a high enzyme loading is desirable, a limiting loading range was described in the literature to avoid the formation of enzyme agglomerates, since it can lead to a decrease in the biocatalyst efficiency by blocking the active site of the immobilized enzyme [1,53].

Chemical Synthesis of racemic 1-benzo[*b*]thiophen-2-yl-ethanol

The synthesis of model substrate and product was performed as earlier reported, see Scheme 1a [46]. Magnesium (117 mg, 7.4 mmol) and one crystal of I_2 were heated for activation in a round bottom flask; 5 mL of diethyl ether were added under argon, followed by methyl iodide (1.1 Eq.) at 0°C. The corresponding 2-formyl derivative (500 mg, 2.8 mmol) dissolved in Et_2O (3 mL) was poured over the resulted stirred solution through a syringe with a long needle under argon at 0°C and after this left to reach the room temperature. The reaction was perfected under stirring overnight at 45°C. For work-up, the reaction was quenched by adding a saturated solution of ammonium chloride (8 mL). The separated aqueous phase was washed with Et_2O (2 × 10 mL). The organic phases were combined and dried using Na_2SO_4, filtered, concentrated and the crude product was purified using column chromatography on silica gel using dichloromethane as eluent, resulting in pure *rac*-**2** as white solid (85% yield).

EKR of racemic 1-benzo[*b*]thiophen-2-yl-ethanol in discontinuous system

The efficiency of the obtained biocatalysts was tested in the enantioselective *O*-transesterification of *rac*-1-benzo[*b*]thiophen-2-yl-ethanol (1.6 mg) with vinyl acetate (2 equiv. for the PLA biocatalyst and 4 equiv. for

the PVA biocatalyst) in 1 mL of *n*-hexane with 0.2 mg immobilized enzyme at 30°C (Scheme 1b) in discontinuous regime. Samples were taken every 30 minutes and analyzed on HPLC (see Figure 7 as example).

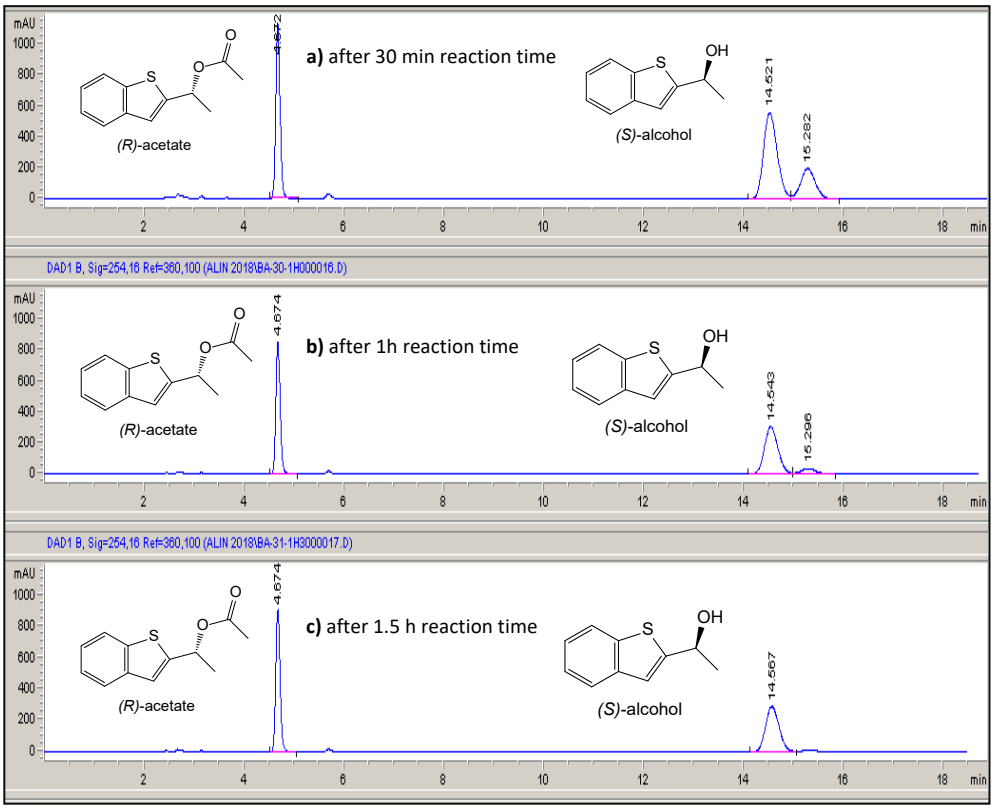

Figure 7. Chromatographic analysis of the EKR of the racemic alcohol with vinyl acetate (**2 equiv.**) in n-hexane at 30°C and 1000 rpm using CaL-B adsorbed on PLA (8%) nanofibers: **a)** chromatographic separation after 30 min; **b)** after 1h and **c)** after 1.5h reaction time.

Recycling experiments

The most promising CaL-B bioconjugate, PLA based, was studied in the enantioselective acylation of racemic 1-benzo[b]thiophen-2-yl-ethanol (8 mg) with vinyl acetate (2 equiv.) (reaction time 1 hour). The reaction was performed 10 consecutive times, the immobilized enzyme being washed with n-hexane (3 × 0.5 mL) after each cycle and immediately used in the next one.

The EKR of *rac*-1-benzo[*b*]thiophen-2-yl-ethanol by *O*-transesterification in continuous system

In order to maximize the productivity of the process, a study regarding the activity and stability of the lipase adsorbed onto the PLA nanofibers in a continuous regime was conducted. The continuous reactor system is presented in Figure 8. Briefly, 49 mg of biocatalyst were introduced as fixed layer in a tubular sealed and thermostated reactor, connected to the HPLC pump. Using a reaction mixture prepared as described in the EKR in discontinuous regime, two process parameters were scanned: flow rate (in the range 0.2–0.5 mL/min), temperature (30, 40, and 50°C) and a constant substrate concentration 8 mg/mL. The reaction progress was monitored taking samples periodically from the effluent and analyzing them by HPLC, until reaching the steady state conditions in the reactor (constant conversion).

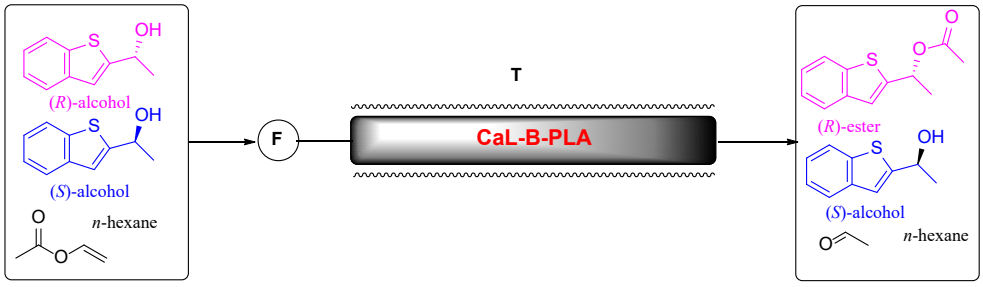

Figure 8. Continuous flow experiments
(49 mg biocatalyst containing 3.71 mg adsorbed CaL-B).

These fibrous structures combine less significant temperature gradients and lower pressure drop in a fixed bed reactor than those in powder form due to the high void fractions or bed porosity.

REFERENCES

1. S. Datta; L. R. Christena; Y. R. S. Rajaram; *Biotech*, **2013**, *3(1)*, 1–9.
2. J. Zdarta; A. S. Meyer; T. Jesionowski; M. Pinelo; *Catalysts*, **2018**, *8*, 92.
3. A. H. Rather; R. S. Khan; T. U. Wani; M. A. Beigh; F. A Sheikh; *Biotechnol. Bioeng.*, **2022**, *119*, 9–33.

4. D. Balogh-Weiser; C. Németh; F. Ender; B. Gyarmati; A. Szilágyi; L. Poppe; Electrospun Nanofibers for Entrapment of Biomolecules. In *Electrospinning Method Used to Create Functional Nanocomposites Films*, 1st ed.; T. A. Tański, P. Jarka, W. Matysiak Eds.; IntechOpen Limited: London, UK, **2018**, DOI: 10.5772/intechopen.76068.
5. MSDS-Europe. https://www.msds-europe.com/ro/ (accessed on 12 June 2022)
6. I. Eş; J. D. G. Vieira; A. C. Amaral; *Appl. Microbiol. Biotechnol*., **2015**, *99(5)*, 2065–2082.
7. A. A. Homaei; R. Sariri; F. Vianello; R. Stevanato; *J. Chem. Biol*., **2013**, *6(4)*, 185–205.
8. M. Dehghani; M. Naseri; H. Nadeem; M. M. Banaszak Holl; W. Batchelor; *J. Environ. Chem. Eng.*, **2022**, *10*, 108686.
9. P. H. Foroushani; E. Rahmani; I. Alemzadeh; M. Vossoughi; M. Pourmadadi; A. Rahda; A. M. Díez-Pascual; *Nanomaterials*, **2022**, *12*, 3426.
10. J.-H. Lin; B.-C. Shiu; P.-W. Hsu; C.-W. Lou; J.-H. Lou; *Polymers*, **2022**, *14*, 4470.
11. J. Wu; Q. Li; G. Su; R. Luo; D. Du; L. Xie; Z. Tang; J. Yan; J. Zhou; S. Wang; K. Xu; *Cellulose*, **2022**, *29*, 5745–5763.
12. Z. Vargas-Osorio; F. Ruther; S. Chen; S. Sengupta; L. Liverani; M. Michálek; D. Galusek; A. R. Boccaccini; *Biomed. Mater*., **2022**, *17*, 045019.
13. V. Korniienko; Y. Husak; J. Radwan-Pragłowska; V. Holubnycha; Y. Samokhin; A. Yanovska; J. Varava; K. Diedkova; Ł. Janus; M. Pogorielov; *Molecules*, **2022**, *27*, 3343.
14. C. G. Spelmezan; L. C. Bencze; G. Katona; F.D. Irimie; C. Paizs; M. I. Tosa; *Molecules*, **2020**, *25*, 350.
15. V. Chauhan; D. Kaushal; V. K. Dhiman; S. S. Kanwar; D. Singh; V. K. Dhiman; H. Pandey; *Front. Bioeng. Biotechnol*., **2021**, *10*, 794411.
16. N. Chuaponpat; T. Ueda; A. Ishigami; T. Kurose; H. Ito; *Polymers*, **2020**, *12(5)*, 1083.
17. K. H. Lam; A. J. Nijenhuis; H. Bartels; A. R. Postema; M. F. Jonkman; A. J. Pennings; P. Nieuwenhuis; *J. Appl. Biomater*., **1995**, *6*, 191–197.
18. M. Shah Mohammadi; M. N. Bureau; S. N. Nazhat; Polylactic Acid (PLA) Biomedical Foams for Tissue Engineering. In *Biomedical Foams for Tissue Engineering Applications,* Woodhead Publishing: Cambridge, UK, 2014; pp. 313–334.
19. G.-L. Gavril; M. Wrona; A. Bertella; M. Świeca; M. Rapa; J. Salafranca; C. Nerín; *Food Chem. Toxicol*., **2019**, *132*, 110662.
20. T. H. Qazi; R. Rai; A. R. Boccaccini; *Biomaterials*, **2014**, *35*, 9068–9086.
21. J. M. Lowen; J. K. Leach; *Adv. Funct. Mater*., **2020**, *30*, 1909089.
22. J. Ou; K. Liu; J. Jiang; D. A. Wilson; L. Liu; F. Wang; S. Wang; Y. Tu; F. Peng; *Small*, **2020**, *16(27)*, 1906184.
23. J.-C. Park; T. Ito; K.-O. Kim; K.-W. Kim; B.-S. Kim; M.-S. Khil; H.-Y. Kim; I.-S. Kim; *Polym. J*., **2010**, *42*, 273–276.
24. A. Kumar; S. S. Han; *Int. J. Polym. Mater. Polym. Biomater*., **2017**, *66(4)*, 159–182.

25. S. A. Braham; E.-H. Siar; S. Arana-Peña; D. Carballares; R. Morellon-Sterling; H. Bavandi; D. de Andrades; J. F. Kornecki; R. Fernandez-Lafuente; *Molecules*, **2021**, *26*, 968.
26. O. Pauli; A. Ecker; A. Cruz-Izquiero; A. Basso; S. Serban; *Catalysts*, **2022**, *12*, 989.
27. G. H. Podrepšek; Ž. Knez; M. Leitgeb; *Front. Bioeng. Biotechnol*., **2022**, *10*, 813919.
28. J. M. Bolivar; J. M. Woodley; R. Fernandez-Lafuente; *Chem. Soc. Rev*., **2022**, *51*, 6251–6290.
29. H. Sánchez-Morán; J. S. Weltz; D. K. Schwartz; J. L. Kaar; *ACS Appl. Mater. Interfaces*, **2021**, *23*, 26694–26703.
30. A. I. Benítez-Mateos; F. Paradisi; Enzyme Engineering: Methods in Molecular Biology. In *Methods in Molecular Biology*, F. Magnani, C. Marabelli, F. Paradisi Eds.; Springer US: New York, NY, USA, **2022**, 2397, pp. 263–276.
31. M. R. Khan; *Bull. Natl. Res. Cent*., **2021**, *45*, 207.
32. M. Solymár; F. Fülöp; L. T. Kanerva; *Tetrahedron Asymmetry*, **2002**, *13*, 2383–2388.
33. J. Uppenberg; N. Öhrner; M. Norin; K. Hult; G. J. Kleyvegt; S. Patkar; V. Waagen; T. Anthonsen; T. A. Jones; *Biochemistry*, **1995**, *34*, 16838–16851.
34. Y. Xie; J. An; G. Yang; G. Wu; Y. Zhang; L. Cui; Y. Feng; *J. Biol. Chem*., **2014**, *289*, 7994–8006.
35. J. C. Rodríguez-Cabello; C. García-Arévalo; I. Quintanilla-Sierra; *Biomimetic Protein Based Elastomers: Emerging Materials for the Future*, Chapter 6, RSC Publishing: London, UK, **2022**.
36. A. Kumar; Krishna; A. Sharma; J. Dhankhar; S. Syeda; A. Shrivastava; *Chemistry Select*, **2022**, *7*, e20220327.
37. P. Qu; M. Kuepfert; E. Ahmed; F. Liu; M. Weck; *Eur. J. Inorg. Chem*., **2021**, *15*, 1420–1427.
38. C. Dourado Fernandes; B. F. Oechsler; C. Sayer; D. de Oliveira; P. H. H. de Araújo; *Eur. Polym. J*., **2021**, *169*, 111–132.
39. K. Lang; H.-B. Quichocho; S. P. Black; M. T. K. Bramson; R. J. Linhardt; D. T. Corr; R. A. Gross; *Biomacromolecules*, **2022**, *23*, 2150–2159.
40. M. Sokołowska; J. Nowak-Grzebyta; E. Stachowska; M. El Frey; *Materials*, **2022**, *15*, 1132.
41. A. Liese; K. Seelbach; A. Buchholz; J. Haberland; Industrial Biotransformations, 2nd ed.; Wiley-VCH: Weinheim, Germany, **2006**, pp. 273–315.
42. A. Basso; S. Serban; *Mol. Catal*., **2019**, *479*, 110607.
43. E. M. Anderson; K. M. Larsson; O. Kirk; *Biocatal. Biotransformation*, **1998**, *16*, 181–204.
44. Q. Wu; P. Soni; M. T. Reetz; *J. Am. Chem. Soc*., **2013**, *135*, 1872–1881.
45. C. Paizs; M.-I. Tosa; V. Bódai; G. Szakács; I. Kmecz; B. Simándi; C. Majdik; L. Nová; F.-D. Irimie; L. Poppe; *Tetrahedron Asymmetry*, **2003**, *14*, 1943–1949.
46. M.-I. Tosa; S. Pilbák; P. Moldovan; C. Paizs; G. Szatzker; G. Szakács; L. Novák; F.-D. Irimie; L. Poppe; *Tetrahedron Asymmetry*, **2008**, *19*, 1844–1852.

47. J. Brem; M.-I. Tosa; C. Paizs; A. Munceanu; D. Matcović-Čalogović; F.-D. Irimie; *Tetrahedron Asymmetry*, **2010**, *21*, 1993–1998.
48. C. G. Spelmezan; G. Katona; L.C. Bencze; C. Paizs; M.-I. Tosa; *React. Chem. Eng*., **2023**, Accepted Manuscript, https://doi.org/10.1039/D2RE00515H.
49. A. M. Isloor; B. Kalluraya; K. S. Pai; *Eur. J. Med. Chem*., **2010***, 45 (2)*, 825–830.
50. C. Bai; S. Ren; S. Wu; M. Zhu; G. Luo; H. Xiang; *Eur. J. Med. Chem*., **2021**, *221*, 113543.
51. M. Seethaler; T. Hertlein; E. Hopke; P. Köhling; K. Ohlsen; M. Lalk; A. Hilgeroth; *Pharmaceuticals*, **2022**, *15(9)*, 1138.
52. R. S. Keri; K. Chand; S. Budagumpi; S. B. Somappa; S. A. Patil; B. M. Nagaraja; *Eur. J. Med. Chem*., **2017**, *138*, 1002–1033.
53. N. R. Mohamad; N. H. C. Marzuki; N. A. Buang; F. Huyop; R. A. Wahab; *Biotechnol. Biotechnol. Equip*., **2015**, *29(2)*, 205–220.
54. P. L. Sóti; D. Weiser; T. Vigh; Z. K. Nagy; L. Poppe; G. Marosi; *Bioprocess Biosyst. Eng*., **2016**, *39(3)*, 449–459.
55. C.-S. Chen; Y. Fujimoto; G. Girdaukas; C. J. Sih; *J. Am. Chem. Soc*., **1982**, *14*, 7294–7299.